infrastructures

MDPI

Article

Strength and Durability Characteristics of Sustainable Pavement Base Course Stabilized with Cement Bypass Dust and Spent Fluid Catalytic Cracking Catalyst

Sajjad E. Rasheed [1], Mohammed Y. Fattah [2,*], Waqed H. Hassan [3] and Mohamed Hafez [4]

[1] Civil Engineering Department, University of Karbala, Karbala 56001, Iraq; sajjad.e@uokerbala.edu.iq or sejjad90@gmail.com
[2] Civil Engineering Department, University of Technology, Baghdad 10056, Iraq
[3] College of Engineering, University of Warith Al-Anbiyaa, Kerbala 56001, Iraq; waqed.hammed@uowa.edu.iq
[4] Department of Civil Engineering, Faculty of Engineering and Quantity Surveying, INTI-International University, Nilai 71800, Malaysia; mohdahmed.hafez@newinti.edu.my
* Correspondence: 40011@uotechnology.edu.iq or myf_1968@yahoo.com

Abstract: This study explores the potential of a composite binder comprising cement bypass dust (CBD) and spent fluid catalytic cracking (FCC) catalyst for sustainable pavement base stabilization. Various CBD/FCC ratios (30:70, 50:50, 70:30) and binder contents (4%, 6%, 8%, 10%) were evaluated through laboratory testing. The 50:50 CBD/FCC mixture demonstrated optimal performance, achieving an unconfined compressive strength (UCS) of 15.6 MPa at 28 days with 10% binder content. The mix exhibited improved stiffness (E50 modulus up to 13,922 MPa) and resistance to degradation under wetting–drying cycles, attributable to synergistic cementitious and pozzolanic reactions. Microstructural analysis revealed a denser matrix, validating the enhanced performance. These findings suggest CBD and FCC, as promising materials for sustainable pavement construction, align with circular economy principles.

Keywords: cement bypass dust; spent fluid catalytic cracking catalyst; sustainable binders; pavement base stabilization; mechanical properties; disaster

Citation: Rasheed, S.E.; Fattah, M.Y.; Hassan, W.H.; Hafez, M. Strength and Durability Characteristics of Sustainable Pavement Base Course Stabilized with Cement Bypass Dust and Spent Fluid Catalytic Cracking Catalyst. *Infrastructures* **2024**, *9*, 217. https://doi.org/10.3390/infrastructures9120217

Academic Editor: Valeria Vignali

Received: 6 November 2024
Revised: 23 November 2024
Accepted: 26 November 2024
Published: 30 November 2024

1. Introduction

The increasing demand for sustainable infrastructure and economic growth necessitate the implementation of sustainable pavement materials and construction practices [1]. One such technique is the use of waste materials and industrial by-products as alternative binders and aggregates in pavement layers. This method could minimize the environmental burden of pavement construction and reduce costs without jeopardizing pavement performance [2,3]. Traditional pavement construction, particularly for flexible pavements, has significant environmental and economic impacts. The production of asphalt and cement, key components in conventional road construction, contributes substantially to global CO_2 emissions. Estimates suggest that the road construction industry is responsible for about 2% of global CO_2 emissions, with cement production alone accounting for about 8% of global CO_2 emissions. Moreover, the extraction of virgin aggregates leads to habitat destruction and landscape alteration. Economically, the rising costs of petroleum-based products and the increasing scarcity of high-quality aggregates are driving up construction and maintenance costs for road infrastructure [4,5].

Recycled materials, such as recycled asphalt pavement and recycled concrete aggregate, have proven to be viable substitutes for virgin aggregate use in the pavements' base and subbase layers—either as partial or full replacements [4,5]. These materials exhibit identical or superior mechanical properties to natural aggregates, and their utilization reduces their impact on the environment since it cuts down the consumption of natural resources

and waste disposal [6,7]. Apart from recycled concrete aggregate (RCA) and reclaimed asphalt pavement (RAP), numerous other waste materials have been explored as possible substitutes for pavement layer materials, such as waste glass [8], waste plastic [9], crushed brick [10], and crumb rubber [11].

An example of a waste material suitable for use in sustainable pavements is cement bypass dust (CBD), which is collected in the cement production process before the feed enters the main burner [12]. Typically, CBD consists mainly of limestone and clay minerals that have not undergone calcination [13]. It may also contain minor amounts of alkali sulfates and free lime [14]. If the dust is not recycled back into the cement production process, it must be disposed of, leading to environmental concerns. However, the calcium carbonate and alumino-silicate phases in CBD can provide binding properties if used with the proper activation [15].

The utilization of cement bypass dust (CBD) in pavement applications has been explored both as a stabilizer and filler material. Early studies demonstrated CBD's potential for soil stabilization, with results showing increased California Bearing Ratio (CBR) values and reduced swell characteristics in treated soils [16]. Subsequent research investigated CBD as a filler in asphalt concrete mixtures, establishing an optimal 5% substitution rate for traditional fillers without compromising mixture properties [17]. More recent work has focused on CBD's role in enhancing the properties of cementitious mixtures, where its high calcium content contributes to strength development through the formation of C-S-H and other hydration products [13]. The chemical reactivity of CBD, particularly its free lime content, makes it especially suitable for stabilization applications [18].

Recent investigations into CBD's performance in stabilization applications have revealed that its effectiveness is closely tied to its chemical composition and particle characteristics. Ref. [19] found that CBD's high alkaline content serves as an effective accelerator for latent hydraulic substances, positively affecting mechanical properties through enhanced hydration reactions. The formation mechanism was further elucidated by [20], who demonstrated that CBD promotes the formation of crucial cementitious phases like belite and mayenite at temperatures as low as 900 °C due to its decarbonated calcium content. This finding is particularly significant for stabilization applications as it indicates CBD's potential to facilitate binding reactions under ambient conditions. Ref. [21] provided additional insight through X-ray diffraction analysis, confirming that CBD contributes to the formation of stable cementitious phases through its interaction with aluminosilicate materials.

Another promising waste material for sustainable pavement construction is spent fluid catalytic cracking catalyst (FCC) residue from oil refineries [22], with an annual production of approximately 160,000 tons and a projected growth rate of 5% [23]. The main components of FCC are silica, alumina, and zeolites, which can contribute to high mechanical performance and durability in construction materials; however, the disposal of this waste also poses environmental issues [22,23]. There have been several proposals for FCC reuse, including extracting valuable metals [24], using it as a supplementary cementitious material [25], incorporating it into geopolymers [23,26], and adding it as a filler material in asphalt mixtures [27]. However, landfilling FCC is still a common disposal method, motivating research into additional applications [28].

Spent FCC has shown promise in various construction applications. Studies on FCC incorporation in asphalt mixtures have demonstrated improvements in high-temperature performance and rutting resistance [29]. The material's unique properties stem from its high alumina and silica content, with research showing that its zeolitic structure and rare earth elements contribute to enhanced material performance [30]. When used in cementitious systems, FCC exhibits significant pozzolanic activity, contributing to the formation of additional calcium silicate hydrate phases that enhance mechanical properties [28]. The material's fine particle size and high specific surface area further promote its reactivity in stabilization applications [27].

The performance characteristics of FCC in construction applications are fundamentally linked to its microstructural properties. Ref. [26] conducted comprehensive analyses

revealing that FCC's effectiveness stems from its high specific surface area and unique particle morphology, which enhance its reactivity in cementitious systems. The material's pozzolanic behavior has been attributed to its amorphous aluminosilicate content, with [30] demonstrating that FCC particles actively participate in strength-developing reactions through surface dissolution and subsequent gel formation. Ref. [23] specifically investigated the role of FCC's zeolitic phases, finding that these components undergo conversion to highly Al-substituted aluminosilicate binders, contributing to enhanced mechanical properties. This mechanistic understanding is crucial as it explains why FCC can effectively participate in stabilization reactions despite being a spent material.

The durability aspects of stabilized base materials have been extensively studied, providing an important context for new stabilizer development. Ref. [10] demonstrated that proper binder selection and content optimization are crucial for achieving long-term performance, particularly in terms of moisture resistance and volume stability. This finding aligns with work by [31], who emphasized the importance of controlling early-age reactions to prevent shrinkage-related issues in stabilized base courses. Studies by [32] on by-product material variability highlight the importance of understanding and controlling material characteristics to achieve consistent performance in stabilized base applications. These considerations are particularly relevant when developing novel stabilizer combinations, as they inform both mix design optimization and performance expectations.

Although there have been several studies examining the use of CBD and FCC individually as substitutes for traditional pavement materials [16,17,22–25,27,28,33], their combination presents a unique opportunity that has not been explored. This gap is particularly significant because the chemical complementarity of these materials suggests potential synergistic effects—CBD's high calcium content could effectively activate FCC's substantial aluminosilicate, potentially leading to enhanced strength development beyond what either material achieves alone. Furthermore, the consumption levels of both waste materials could be optimized—while previous studies focused on using each material separately at higher replacement rates, their combination could achieve better performance with lower total waste material content, making the approach more economically viable. The materials are often generated in geographical proximity, with cement plants and oil refineries frequently located in industrial zones, reducing transportation costs and the environmental impact of the proposed solution. Unlike traditional supplementary cementitious materials like fly ash or slag, both CBD and FCC are currently underutilized in most regions, making their combination a truly novel approach to waste material valorization in pavement applications. This research addresses these opportunities by systematically investigating the combined use of CBD and FCC as a stabilizing agent, with the potential to establish a new pathway for sustainable pavement base construction while simultaneously addressing two significant industrial waste challenges.

The aim of this study is to evaluate the efficacy of a composite binder comprising cement bypass dust (CBD) and spent fluid catalytic cracking (FCC) catalyst for stabilizing granular base layers in flexible pavements, with a focus on developing a sustainable alternative to conventional stabilization methods. The objectives of this research are as follows:

1. Formulate and characterize stabilized base specimens using various CBD/FCC ratios and binder contents.
2. Assess the mechanical properties of the stabilized specimens through unconfined compressive strength testing and stress–strain analysis.
3. Evaluate the durability of optimized mixtures via wetting–drying cycle testing.
4. Analyze the microstructural characteristics of the stabilized materials using SEM, XRD, and EDS techniques.
5. Determine the optimal CBD/FCC ratio and binder content for achieving superior mechanical performance and durability.
6. Compare the performance of the CBD-FCC stabilized base material against conventional stabilization methods to assess its viability as a sustainable alternative.

7. These objectives are designed to evaluate the potential of CBD-FCC as a novel, eco-friendly binder for pavement base stabilization, addressing both engineering performance and environmental sustainability concerns in road construction.

2. Materials

2.1. Unbound Base Course

The unbound granular base (UGB) material used in this study was crushed gravel aggregate procured from local quarries supplying an asphalt pavement plant. The gravel was crushed, washed, and screened to meet specifications for base course aggregates as per Iraqi standard R7 [34]. The grain size distribution of the crushed gravel aggregate is presented in Figure 1. The aggregate was broadly graded between the 3/2 in. and No. 200 sieves, with 10% passing the No. 200 sieve. The coarse fraction retained on the No. 4 sieve was 55% gravel content. The fine fraction passing the No. 4 sieve and retained on the No. 200 sieve was 35%. The fines passing the No. 200 sieve comprised 10% silt/clay-sized particles. This distribution allows for an adequately graded base course material with sufficient fines for particle interlock while preventing excessive amounts that can impact stability.

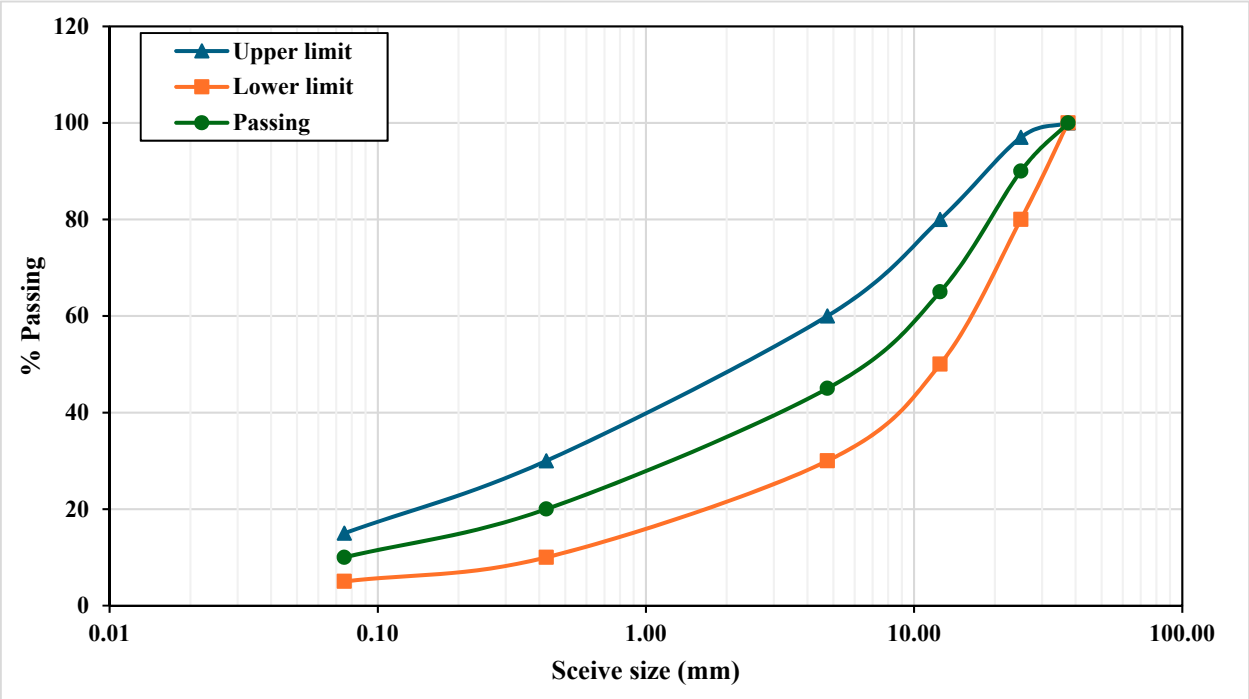

Figure 1. Particle size distribution of UGB.

Atterberg limits testing on the fines indicated a liquid limit of 14%; Modified Proctor compaction testing resulted in a maximum dry density of 2.39 g/cm^3 at an optimum moisture content of 5.4% by weight. The California bearing ratio after 4 days of soaking was 83%. The Los Angeles abrasion loss for the crushed aggregate was 29%. Unconfined compressive strength testing indicated a strength of 580 kPa for untreated specimens compacted to 100% of modified Proctor densities. All physical and engineering properties tested met specifications for a base course aggregate material as set out in Iraqi standard R7-2003 [34], as summarized in Table 1.

Table 1. Properties of UGB.

Test	Result	Requirements	Test Standard
SO_3 content (%)	1.14%	<5%	B.S. 1377-3-2018 [35]
TSS content (%)	2.12%	<5%	B.S. 1377-3-2018 [35]
Gypsum content (%)	2.3%	<5%	ASTM D 2974-20 [36]
Liquid limit (%)	14	<25%	AASHTO T89-68 [37]
Plasticity Index (%)	-	<4%	AASHTO T90-70 [38]
California Bearing Ratio (%)	83%	>80%	ASTM D 1883 [39]
L.A. abrasion loss (%)	32.10%	<45%	ASTM C 131/131 M-20 [40]
MDD (g/cm^3)	23.9 kN/m^3	-	ASTM D 1557-12 R21 [41]

2.2. Cement Bypass Dust (CBD)

The cement bypass dust used in this study (Figure 2) was provided by the Lafarge cement factory located just outside Karbala city in Iraq. Chemical and mineralogical characterization of the cement bypass dust (CBD) was carried out through X-ray fluorescence (XRF) spectrometry and X-ray diffraction (XRD) analyses. XRF results shown in Table 2 indicate a predominance of calcium oxide at 84.2% by mass, suggesting the CBD consists primarily of unreacted calcium compounds leftover from the cement clinkering process. This is verified by the significant calcite ($CaCO_3$) peaks observed in the XRD pattern shown in (Figure 3) [20,21]. The CBD also contains silicon dioxide, confirmed by the presence of quartz (SiO_2) diffraction peaks, likely originating from the clay and shale deposits used as inputs for cement production. Additional minor fractions of phosphates and alkali compounds are detected, which may enter the CBD stream due to incomplete volatilization in the kiln. The high amorphous calcium-rich content indicates the potential reactivity of this CBD with pozzolanic aluminosilicate materials to form strengthened cementitious gels. Prior to use, the CBD was passed through a #325 (0.045 mm) sieve to ensure consistent particle size distribution and enhance its reactivity potential. This processing step standardizes the material's fineness, which is crucial for its cementitious properties as finer particles provide greater surface area for hydration. The fine particle size of CBD promotes a more uniform distribution and ensures optimal interaction with other mixture components.

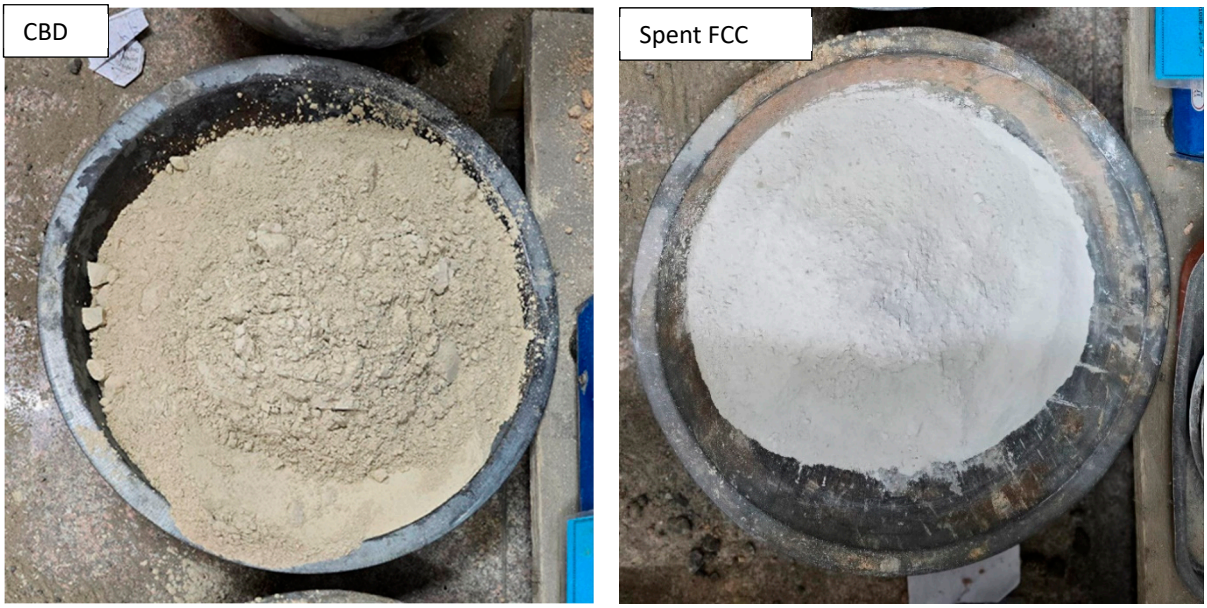

Figure 2. Waste materials utilized in the present study.

Table 2. Chemical composition of CBD.

Oxides	Content (%)
CaO	84.2
SiO_2	3.6
K_2O	3.8
Fe_2O_3	4.9
Al_2O_3	0.3
Others	3.2

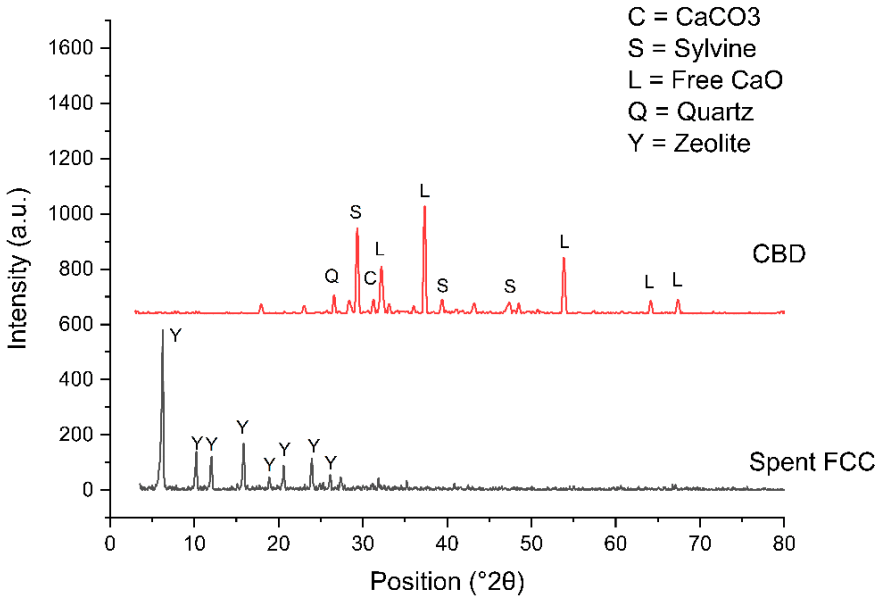

Figure 3. X-ray diffraction of CBD and FCC.

2.3. Spent Fluid Catalyst Cracking (FCC)

Spent FCC material (Figure 2) was supplied by Karbala City's oil refinery. Characterization of spent FCC indicated that it contained elevated levels of silica and alumina, as quantified by X-ray fluorescence (XRF) spectroscopy in Table 3. The majority of silica is present in an amorphous phase, as evidenced by X-ray diffraction (XRD) analysis (Figure 3), which revealed a high baseline elevated over a wide angular range. The significant X-ray amorphous hump indicates the original zeolite crystalline (zeolite Y) fraction has almost entirely degraded into an aluminosilicate glass upon exposure to hydrocarbon feedstocks at high temperatures in the FCC unit. However, some sharp diffraction peaks are still observed in the XRD pattern, corresponding to meaningful zeolite crystallinity persisting that did not completely break down under hydrothermal reaction conditions. High levels of structural alumina are also inherent to both the amorphous and zeolitic crystalline components, as confirmed by XRF elemental analysis. Other metals originating from matrix components and the fluidized bed reactor system used in the FCC unit are present at much lower levels. The spent FCC material was also processed through a #325 (0.045 mm) sieve before incorporation into the mixtures. This standardization of particle size maximizes the material's pozzolanic activity, as previous research has shown that finer FCC particles demonstrate enhanced reactivity in cementitious systems. The controlled particle size ensures consistent material performance and promotes efficient chemical reactions within the stabilized base matrix.

Table 3. Chemical composition of FCC.

Oxides	Content (%)
Si_2O_3	49.9
Al_2O_3	28.9
TiO_2	7.5
Fe_2O_3	6
La_2O_3	2.4
Others	5.3

2.4. Methodology

The experimental methodology evaluated a composite binder of cement bypass dust (CBD) and spent fluid catalytic cracking (FCC) catalyst for pavement base stabilization. Three FCC/CBD ratios (30:70, 50:50, 70:30) were investigated to balance CBD's cementitious properties and FCC's pozzolanic activity, maximizing their synergistic reactions. Ratios with higher dominance of either material, such as 90:10 or 10:90, were avoided due to potential performance limitations. Excess CBD could lead to reduced pozzolanic activation, while excessive FCC might lack sufficient calcium to support hydration reactions. The chosen ratios represent a practical range that ensures effective chemical interaction based on material feasibility for real-world applications. Unconfined compressive strength tests at 7 days of curing determined the optimal ratio. Four binder percentages of this optimal ratio underwent comprehensive characterization, including mechanical performance, durability, and microstructural analyses. Figure 4 shows the flowchart of the experimental program for determining optimal binder composition and content for enhanced pavement base performance. Table 4 presents the mixing proportions and sample identifications for all combinations.

Table 4. Mixing proportions and sample identification.

ID	Binder (%)	CBD/FCC	CBD (g)	FCC (g)	UGB (g)	Water (g) *	Total (g)
M01	4	30:70	48	112	4000	233	4393
M02	4	50:50	80	80	4000	233	4393
M03	4	70:30	112	48	4000	233	4393
M04	6	30:70	72	168	4000	246	4486
M05	6	50:50	120	120	4000	246	4486
M06	6	70:30	168	72	4000	246	4486
M07	8	30:70	96	224	4000	260	4580
M08	8	50:50	160	160	4000	260	4580
M09	8	70:30	224	96	4000	260	4580
M10	10	30:70	120	280	4000	278	4678
M11	10	50:50	200	200	4000	278	4678
M12	10	70:30	280	120	4000	278	4678

* Values obtained from modified Proctor test.

2.5. Sample Preparation

The optimum moisture content for the mixes was determined based on modified Proctor compaction testing per [41]. The crushed gravel aggregates, cement bypass dust (CBD), and spent fluid catalytic cracking catalyst (FCC) powders were dry-mixed thoroughly in predetermined proportions. A 30 L capacity laboratory mechanical mixer was employed to achieve homogeneity of the blended mixture along with the specified water content. The resulting mixtures were then compacted in 101 mm inner diameter steel cylinder molds having 200 mm height. A modified 4.54 kg Proctor hammer was utilized for compaction by applying 25 blows uniformly distributed in 5 layers. This enabled replication of field densities, with the compacted samples achieving a minimum of 95% modified Proctor density. The prepared stabilized base samples, representing different CBD/FCC ratios and binder contents, were extruded 24 h after compaction and cured in a laboratory environ-

ment where ambient room temperature was maintained at 25 ± 2 °C using air conditioning. Specimens were stored on laboratory shelves and covered with plastic sheets to minimize moisture loss during curing. The ambient temperature was monitored daily using laboratory thermometers. For wetting–drying cycles, specimens were subjected to controlled temperature conditions during the drying phase using a thermostatically controlled oven maintained at 71 ± 2 °C for 42 h. The wetting phase was conducted at room temperature (25 ± 2 °C) for 5 h using tap water. All strength tests were performed at room temperature after specimens were removed from their storage location. The laboratory conditions were selected to represent typical ambient curing environments that would be encountered in field applications. The sample preparation sequence is presented in Figure 5.

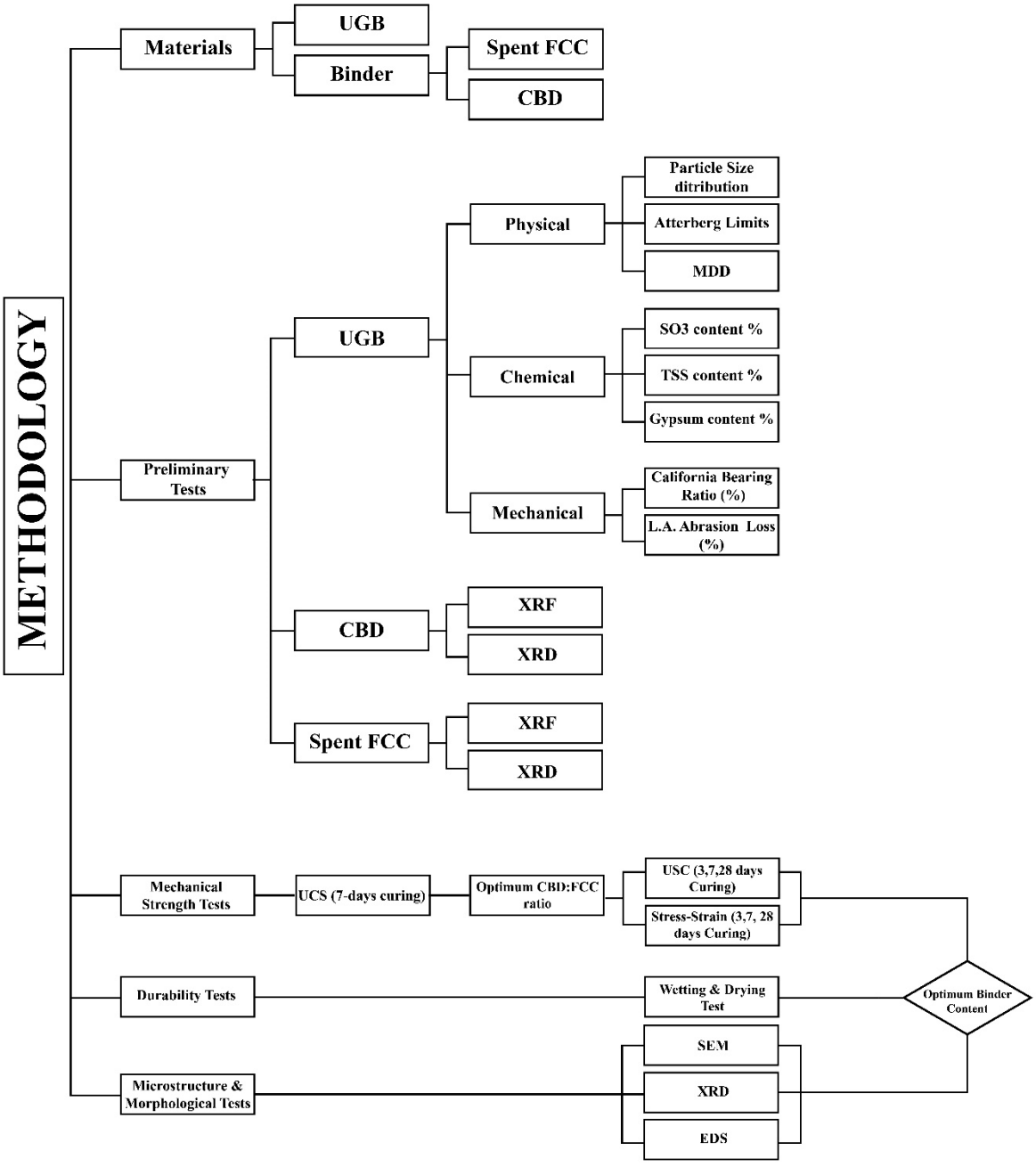

Figure 4. Flowchart of the experimental program.

Figure 5. Sample preparation sequence. (**a**) UGB retained at specified sieves, (**b**) prepared mix, (**c**) dry mix, (**d**) wet mix, (**e**) compacted samples, and (**f**) extruded samples.

2.6. Unconfined Compressive Strength

The ASTM D1633M-17 standard test method [42] was adhered to for quantifying the unconfined compressive strength (UCS) of the compacted samples after curing. As per specifications, the rate of strain application was maintained between 1% and 2% per minute during axial loading of cylinder specimens using a compression testing machine. Three duplicate samples for each CBD-FCC blend were tested at 7 days of curing. The maximum axial load at failure recorded by the machine-integrated data logger was used to compute the UCS as the ratio of failure load to the initial cross-sectional area resisting the compression. The optimum CBD-FCC blend selected based on the UCS test was then used for the rest of the samples to be tested at 3, 7, and 28 days.

2.7. Wetting–Drying Exposure

Ref. [43] details the test method for assessing the durability of compacted soil–cement mixtures through cycles of wetting and drying. In this procedure, soil–cement specimens are molded and cured. They are then subjected to 12 cycles where each cycle involves immersing the specimens in water for 5 h and oven-drying them at 71 °C (160 °F) for 42 h. After each drying phase, the specimens are brushed with a wire scratch brush specified by the standard: it has six sets of stiff steel wires (bristles) with 14 wires per set, each wire being 0.33 mm in diameter. The brush is applied manually with a force of approximately 13.5 N to remove loose material. The mass loss of the specimens after brushing is measured after each cycle. The cumulative mass loss indicates the material's resistance to deterioration from wetting and drying, aiding in determining its suitability for construction purposes.

3. Results and Discussion

3.1. Compaction Test Result

The moisture–density relationship of the stabilized mixes was investigated using the modified Proctor compaction test (ASTM D1557). The tests were conducted on mixes with binder contents of 4%, 6%, 8%, and 10%. As shown in Figure 6, the optimum moisture content increased consistently with higher binder content, from 5.6% at 4% binder to 6.3% at 10% binder. This trend is attributed to the higher water demand of the fine CBD and FCC particles compared to the granular base material. Conversely, the maximum dry density showed a slight decreasing trend from 23.8 kN/m^3 to 22.9 kN/m^3 as binder content increased from 4% to 10%. This reduction in density can be explained by the lower specific gravity of the binder materials compared to the base aggregate. Table 5 presents the optimum moisture content (OMC) and maximum dry density (MDD) values for each binder content and Figure 6 presents the compaction curves of the stabilized mixes.

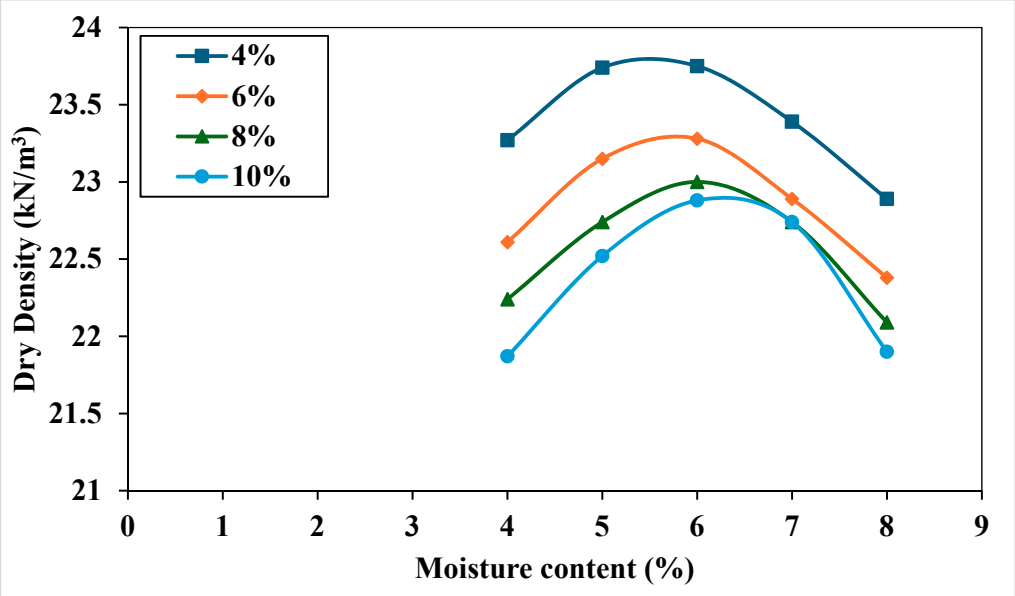

Figure 6. Compaction curves of the stabilized mixes with varying binder contents.

Table 5. Optimum moisture content (OMC) and maximum dry density (MDD) of the stabilized mixes.

Binder Content	O.M.C (%)	MDD (kN/m^3)
4%	5.6	23.8
6%	5.8	23.3
8%	6	23
10%	6.3	22.9

3.2. Unconfined Compressive Strength (UCS)

The unconfined compressive strength (UCS) results of the three stabilized granular base mixes at different binder addition percentages and 7 days of curing are presented in Figure 7.

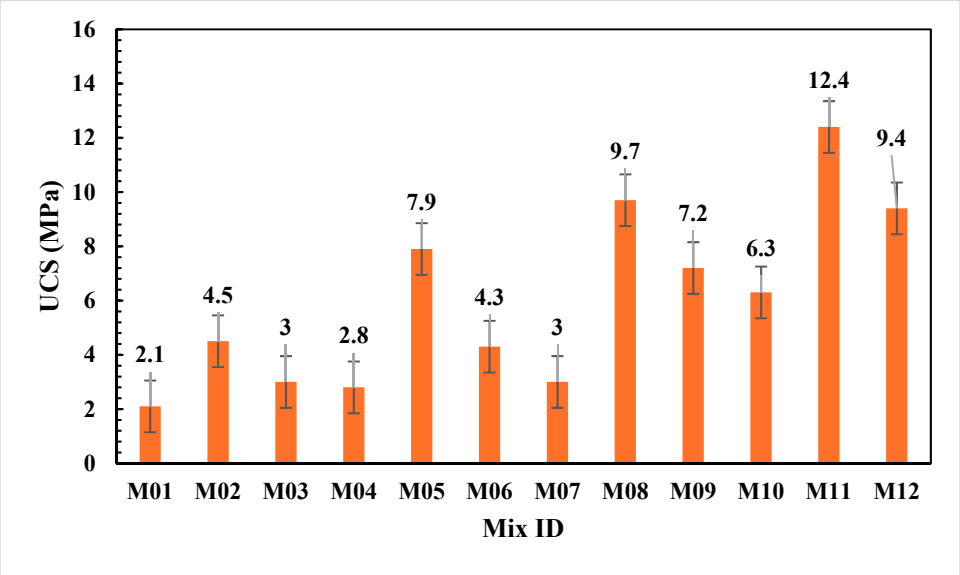

Figure 7. UCS values for different FCC/CBD mixes.

The results demonstrate the significant influence of both binder content and CBD/FCC proportions on strength development. The 50:50 CBD/FCC mixes (M02, M05, M08, M11) exhibit consistently superior UCS values, progressing from 4.5 MPa at 4% binder content to 12.4 MPa at 10% binder content. This marked performance advantage stems from the synergistic interaction between FCC's pozzolanic reactivity and CBD's cementitious properties, fostering the formation of a dense, interconnected matrix [44,45]. The balanced proportions enable optimal chemical interaction between the materials, maximizing their respective contributions to strength development [46]. The 30:70 CBD/FCC mixes (M01, M04, M07, M10) demonstrate notably lower strength development, with values ranging from 2.1 MPa to 6.3 MPa. This performance limitation reflects insufficient CBD content for proper activation of the FCC's pozzolanic potential. Particularly telling is the irregular strength progression until reaching 10% binder content, where a significant jump to 6.3 MPa occurs, suggesting that high binder contents are required to compensate for the suboptimal material ratio [47].

The 70:30 CBD/FCC mixes (M03, M06, M09, M12) achieve intermediate performance, with UCS values ranging from 3.0 MPa to 9.4 MPa. While showing more consistent strength progression than the 30:70 ratio, these mixes still fall short of the 50:50 performance. The most substantial strength gain occurs between 6% and 8% binder content, reaching 7.2 MPa, indicating a critical threshold where sufficient FCC is available for reaction with the abundant CBD. The bar charts shown in Figure 8 present the unconfined compressive strength (UCS) results for a stabilized base material containing 50% CBD and 50% FCC at various binder addition percentages (4%, 6%, 8%, and 10%) and curing periods (3, 7, and 28 days).

The UCS values show a consistent increasing trend with both higher binder content and longer curing times. At 3 days of curing, the UCS ranges from 4.2 MPa at 4% binder content to 6.7 MPa at 10% binder content. This early-age strength development can be attributed to the rapid pozzolanic reactions of the FCC, which contribute to the formation of cementitious compounds [48]. The 7-day UCS values demonstrate significant improvement compared to the 3-day results, with the mix achieving 4.5 MPa at 4% binder content and

12.4 MPa at 10% binder content. This strength gain is likely due to the ongoing hydration and pozzolanic reactions, resulting in a denser cementitious matrix [49]. At 28 days of curing, the UCS values range from 8 MPa (4% binder) to 15.6 MPa (10% binder), indicating the long-term strength development of the 50% CBD:50% FCC mix. The prolonged curing allows for the completion of the pozzolanic reactions and the formation of a robust, interconnected cementitious matrix [50].

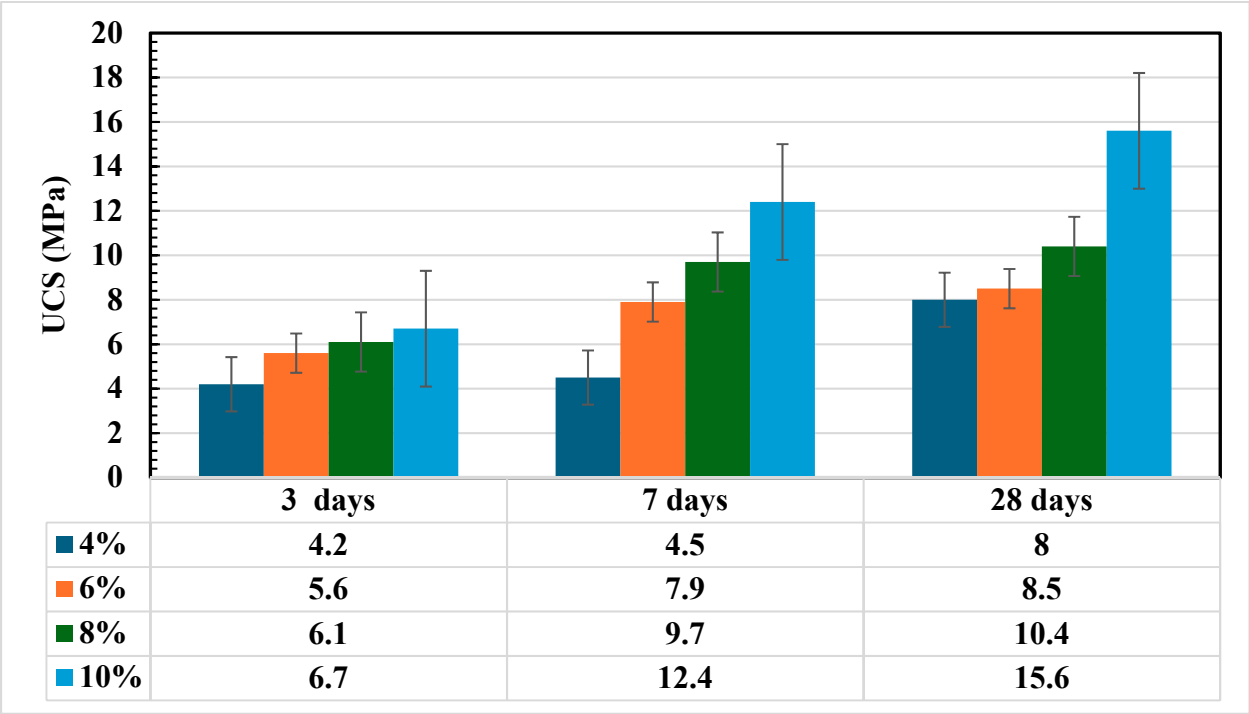

	3 days	7 days	28 days
4%	4.2	4.5	8
6%	5.6	7.9	8.5
8%	6.1	9.7	10.4
10%	6.7	12.4	15.6

Figure 8. UCS values for different curing periods.

The present study's findings can be contextualized within the broader field of pavement base stabilization research. Ref. [51] investigated the stabilization of different recycled asphalt pavement (RAP) to aggregate ratios using varying cement contents. Their results demonstrated that for each percentage increase in Portland cement content, the unconfined compressive strength (UCS) of stabilized SP-SC and GW-GC layers increased by approximately 376 kPa and 410 kPa, respectively. This linear relationship between cement content and strength gain provides a useful benchmark for evaluating alternative stabilization methods.

In comparison, Ref. [52] explored an innovative geopolymer stabilizer composed of calcium carbide residue (CCR) activated by linear alkyl benzene sulfonic acid (LABSA). Their approach yielded significant UCS improvements, with increases ranging from 213% to 321% at 7 days and 233% to 370% at 28 days, relative to untreated aggregate. The influence of curing time was notable, with UCS increases of 9.2%, 14.2%, and 15.3% observed between 7 and 28 days for short-term rainfall, continual fine weather, and warm conditions, respectively. However, strength development plateaued after 28 days, with gains not exceeding 3% across all curing conditions up to 60 days. These findings highlight the importance of considering both short-term strength development and long-term stability in evaluating novel stabilization techniques.

The chart clearly illustrates the positive influence of both binder content and curing time on the UCS of the stabilized base material. The synergistic effect of the CBD and FCC, with their respective cementitious and pozzolanic properties, contributes to the impressive strength gains observed. The high UCS values at 28 days suggest that the 50% CBD:50% FCC mix has the potential to create a durable and high-performance stabilized base material for sustainable pavement applications.

3.3. Stress–Strain Behavior and E50 Modulus

The stress–strain behavior of the stabilized base material containing 50% CBD and 50% FCC was evaluated at 3, 7, and 28 days of curing for binder percentages of 4%, 6%, 8%, and 10%. Figure 9 presents the stress–strain curves for samples cured for 3, 7, and 28 days.

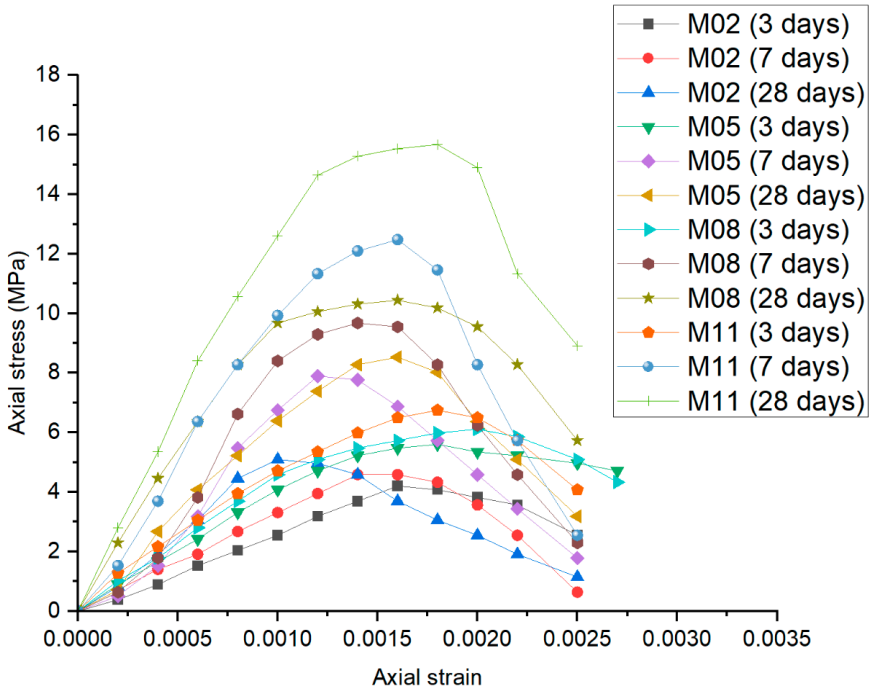

Figure 9. Stress–strain curves for CBD-FCC treated samples.

Stress–strain analysis of the stabilized base material containing 50% CBD and 50% FCC was evaluated at different curing periods. The secant modulus at 50% of the ultimate stress (E50) was determined from stress–strain curves to characterize material stiffness. As shown in Table 6, E50 values demonstrated consistent increases with both curing time and binder content, progressing from 2547 MPa for M02 at 3 days to 13,922 MPa for M11 at 28 days. This substantial improvement in stiffness, particularly pronounced in M11, indicates progressive formation of cementitious products through hydration and pozzolanic reactions [53]. The synergistic effect of CBD and FCC contributes to both short-term and long-term stiffness development. The CBD component provides early stiffness through hydration reactions, while the FCC enhances long-term performance through pozzolanic reactions, similar to findings reported by [25] in their study of FCC as a supplementary cementitious material. The observed trends in E50 evolution demonstrate the effectiveness of the CBD-FCC blend in improving the mechanical properties of the stabilized base material, with results comparable to those reported for other cement-based and pozzolanic stabilized materials [54]. The E50 results are summarized in Table 6.

Table 6. E50 results.

MixID	3-Day Curing	7-Day Curing	28-Day Curing
M02	2547 MPa	3274 MPa	4982 MPa
M05	3370 MPa	6503 MPa	7005 MPa
M08	4576 MPa	8140 MPa	8716 MPa
M11	5025 MPa	10,566 MPa	13,922 MPa

CBD is rich in calcium oxide (CaO) and alkalis, which promote pozzolanic and cementitious reactions when combined with other materials like lime or fly ash. This contributes to improved early and long-term strength. Partial replacement of traditional binders with CBD enhances compressive strength, making it suitable for base course applications.

Spent FCC catalyst contains alumina (Al_2O_3) and silica (SiO_2), which exhibit pozzolanic properties. These properties improve the microstructure of the base course material, leading to higher strength over time. The addition of spent FCC catalysts often increases flexural strength, making the pavement less susceptible to cracking under load.

CBD improves durability by reducing the permeability of the base course, which protects against moisture infiltration and freeze–thaw cycles. However, the high alkali content in CBD may pose risks of alkali–silica reaction (ASR) if reactive aggregates are present. Proper mix design and curing conditions are necessary to mitigate this.

Spent FCC catalyst enhances durability by densifying the matrix and reducing pore sizes, thereby increasing resistance to environmental degradation (e.g., moisture, chloride penetration). It also improves resistance to chemical attack due to its inert nature once stabilized.

3.4. Wetting and Drying Test

The weight loss during the wetting and drying cycles, calculated as a percentage of the specimen's original oven-dry mass [43], increases with increasing cycles for all binder percentages (Figure 10). The rate of weight loss, however, is notably lower for higher binder percentages (8% and 10%) compared to lower binder percentages (4% and 6%). This observation suggests that increasing the binder content enhances the mixture's resistance to degradation, likely due to the formation of a more robust and interconnected cementitious matrix. The increase in weight loss with increasing cycles is consistent with the results of [50,51], which attribute this behavior to the gradual breakdown of the soil–cement bonds and the loss of fine particles during the wetting and drying process.

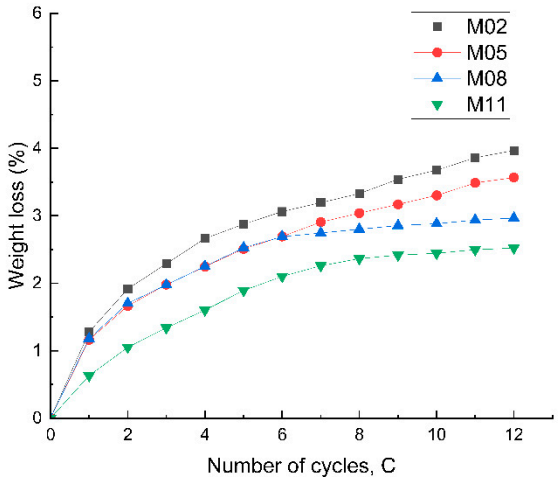

Figure 10. Weight loss due to consecutive wetting and drying cycles.

The effects of wetting and drying cycles on the strength and durability of a Cement Bypass Dust (CBD) and Spent FCC Catalyst-treated sustainable pavement base course are significant, as these cycles mimic the environmental stresses experienced by pavements. Early Strength Loss: Repeated wetting and drying cycles can lead to microcracking, reducing the cohesion between particles and causing minor reductions in compressive and flexural strength.

The calcium and alkali content in CBD may react with water during wetting, further activating pozzolanic and cementitious reactions. This can sometimes offset initial strength loss, resulting in stabilization and strength recovery over long periods.

FCC catalysts enhance the matrix's density and pozzolanic properties, making it more resistant to the strength-reducing effects of wetting and drying.

Sustained Performance: The alumina and silica content in the FCC catalyst enhances interparticle bonding, allowing the base course to retain more of its strength under cyclic wetting and drying.

Repeated wetting and drying cycles can lead to gradual expansion and contraction, increasing porosity and susceptibility to moisture ingress. The pozzolanic reaction helps maintain integrity and minimize the formation of shrinkage cracks caused by drying.

The trend of volume loss also increased as the number of cycles increased, as indicated in (Figure 11), but at a lower rate for higher binder percentages. This outcome shows that increasing the binder content improves the volume stability of the mixture, which is essential for maintaining the structural properties and performance of the pavement's base layer. The reduced volume loss at a higher binder percentage is due to the presence of some cementitious products, such as calcium silicate hydrate and calcium aluminate hydrate, that enhance the strength and dimensional stability of the mixture [55]. The hydration products from the reaction between the binder material and the soil particles fill the pores within the soil–cement matrix, making the structure more dense and resistant to moisture-induced volume changes.

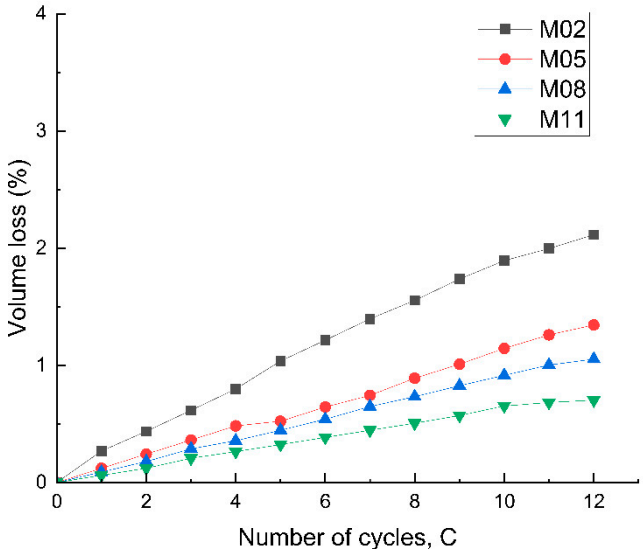

Figure 11. Volume loss due to consecutive wetting and drying cycles.

Furthermore, the reduced weight and volume loss at higher binder percentages can also be attributed to the pozzolanic reactions of spent FCC, which refine the microstructure of the cementitious matrix and enhance the mixture's durability [56]. The pozzolanic reaction between the silica and alumina in spent FCC and the calcium hydroxide produced during cement hydration leads to the formation of additional C-S-H and C-A-H, further strengthening the soil–cement matrix and improving its resistance to deterioration caused by wetting and drying cycles.

Figure 12 reveals progressive deterioration of cement bypass dust (CBD) and spent fluid catalytic cracking catalyst (FCC)-stabilized base course samples with increasing wetting–drying cycles. Cracking, spalling, and material loss become more pronounced, aligning with observations by [56] that cyclic wetting–drying causes initial microstructural changes and degradation [43].

Rasul et al. [57] found that samples subject to wetting and drying exhibited significantly greater permanent deformation and had lower values of resilient modulus than those that were not subject to wetting and drying.

However, higher total CBD-FCC binder contents (M11) provide improved resistance to degradation compared to lower contents (M02), even after 12 cycles. This suggests that

increased binder content facilitates more extensive pozzolanic reactions that counteract the deleterious effects of wetting–drying [58]. The results demonstrate the importance of sufficient stabilizer content for the long-term durability of sustainable pavement bases under severe environmental conditions.

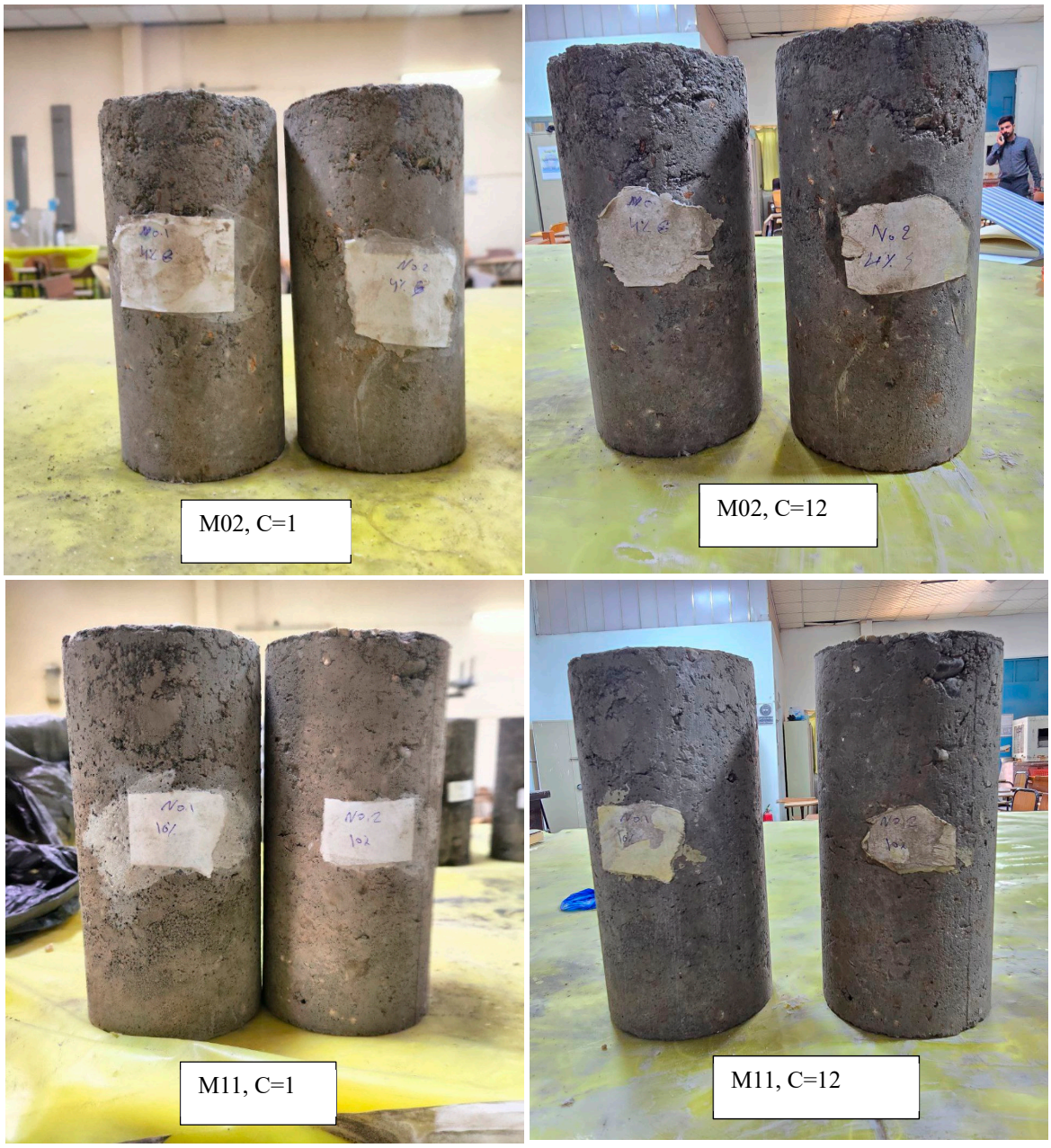

Figure 12. CBD-FCC treated samples subjected to wetting and drying cycles.

3.5. Microstructural and Morphological Analysis

Figure 13 presents a comparative Field Scanning Electron Microscopy (FeSEM) analysis of the microstructural characteristics of the M02 and M11 samples at two different scales. These samples were specifically selected as they represent the lower and upper limits of the binder content range investigated in this study and exhibited the most significant differences in mechanical strength and durability. The M02 sample shows a predominantly smooth, planar surface morphology with minimal topographical variation. At 5 µm magnification, the surface exhibits a relatively uniform texture with sparse, isolated crystalline deposits appearing as bright spots on the surface. The 20 µm view reveals occasional

clusters of crystalline formations but maintains a largely continuous matrix with limited evidence of hydration product development, suggesting restricted chemical interaction between the binder components at 4% content.

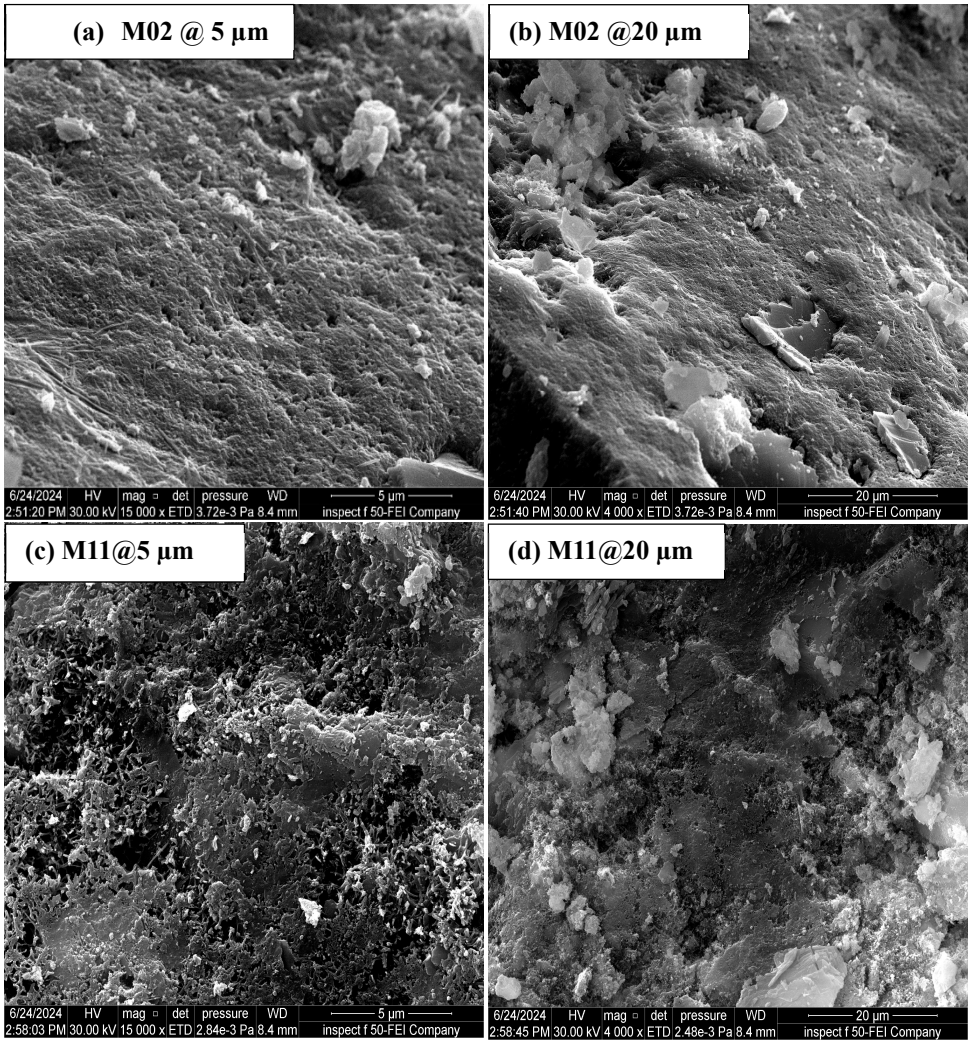

Figure 13. FeSEM test for the stabilized base course samples: (**a**) M02 @ 5 µm, (**b**) M02 @ 20 µm, (**c**) M11 @ 5 µm, (**d**) M11 @ 20 µm.

M11 micrographs display dramatically different features, characterized by a highly textured, honeycomb-like structure. At 5 µm, the surface shows an intricate network of fine, needle-like formations and irregular micro-pores, indicating extensive development of C-S-H and C-A-H phases. The 20 µm magnification reveals a complex, three-dimensional structure with abundant crystalline clusters and a significantly rougher surface topography. This microstructural evolution demonstrates more complete hydration and pozzolanic reactions at 10% binder content, creating a denser, more interconnected matrix that explains the superior strength values observed in mechanical testing.

The XRD patterns shown in Figure 14 comparing M02 (4% binder) and M11 (10% binder) samples reveal distinct mineralogical differences. M11 exhibits stronger and more numerous peaks for C-S-H phases (marked as S) at 2θ angles of 21°, 29.5°, 42°, 47°, and 50°, indicating enhanced formation of calcium silicate hydrate gel. The presence of well-defined C-A-H peaks at 40°, 45°, and 60° in M11 demonstrates significant aluminate phase development, which is notably absent in M02. The calcite ($CaCO_3$) peak at 30° shows higher intensity in M02, suggesting more unreacted calcium-rich phases. The reduced calcite peak intensity coupled with increased C-S-H and C-A-H peaks in M11 provides direct evidence

of more extensive pozzolanic reactions at higher binder content. The sharper peak definition in M11, particularly for the C-S-H phases, indicates better crystallinity and more complete hydration reactions [59,60], explaining the superior mechanical performance observed in strength testing. The M02 sample generally exhibits broader peaks with higher full-width at half-maximum intensity (FWHM) values, indicating smaller crystallite sizes or higher microstrains [61].

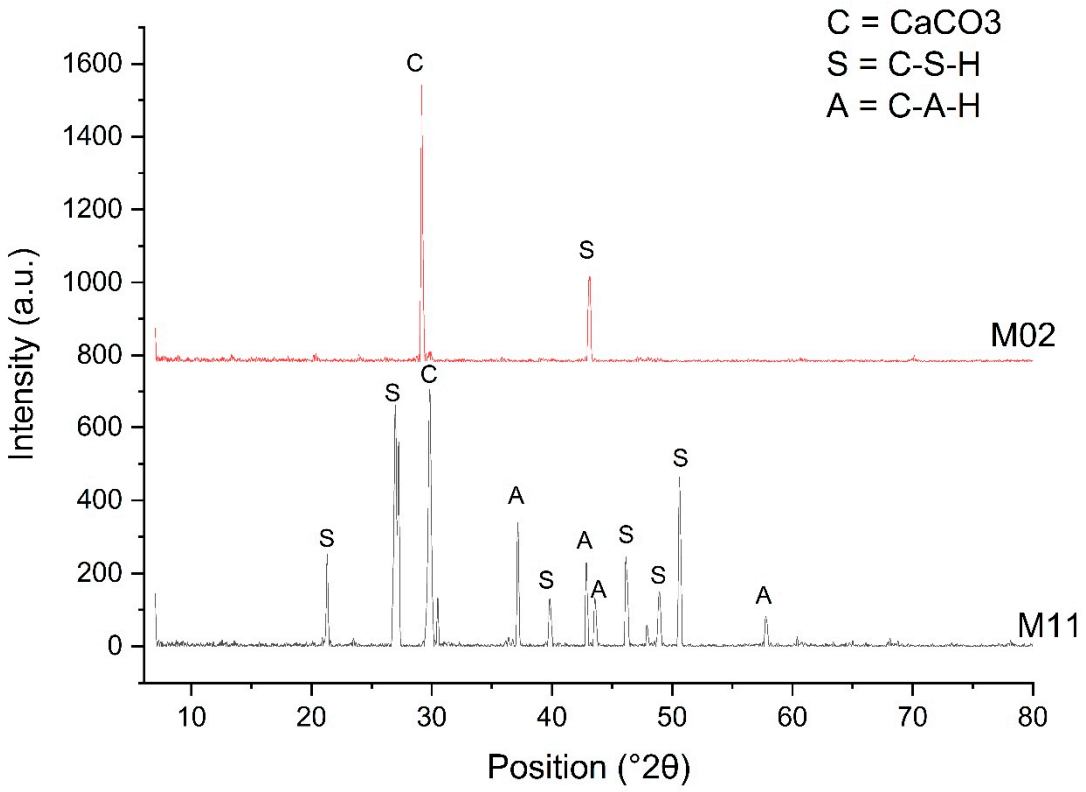

Figure 14. XRD patterns for M02 and M11 samples after UCS test at 28 days.

The Energy-Dispersive X-ray Spectroscopy (EDS) data for the M02 and M11 samples are presented in Figure 15. The M11 sample exhibits increased oxygen and silicon content, demonstrating enhanced hydration and pozzolanic reactions. A decrease in calcium content lowers the Ca/Si ratio, promoting longer chain silicates in the calcium silicate hydrate (C-S-H) gel [62]. This modified (C-S-H) structure, characterized by a denser and more interconnected matrix, directly contributes to the improved strength and durability observed in the 10% binder mix [63]. These compositional changes elucidate the chemical mechanisms underlying the superior performance of the higher binder content in sustainable pavement base stabilization.

Both CBD and FCC catalysts promote the recycling of industrial byproducts, reducing landfill waste and environmental pollution.

Their use reduces the demand for virgin materials and the carbon footprint associated with conventional binder production.

The effectiveness of CBD and FCC catalysts depends on their proportions in the mix. Excessive CBD can lead to brittleness, while too much FCC catalyst may affect workability. Careful assessment of the compatibility of these byproducts with other pavement materials is crucial. CBD, in particular, may contain heavy metals. Ensuring minimal leaching is critical for environmental safety.

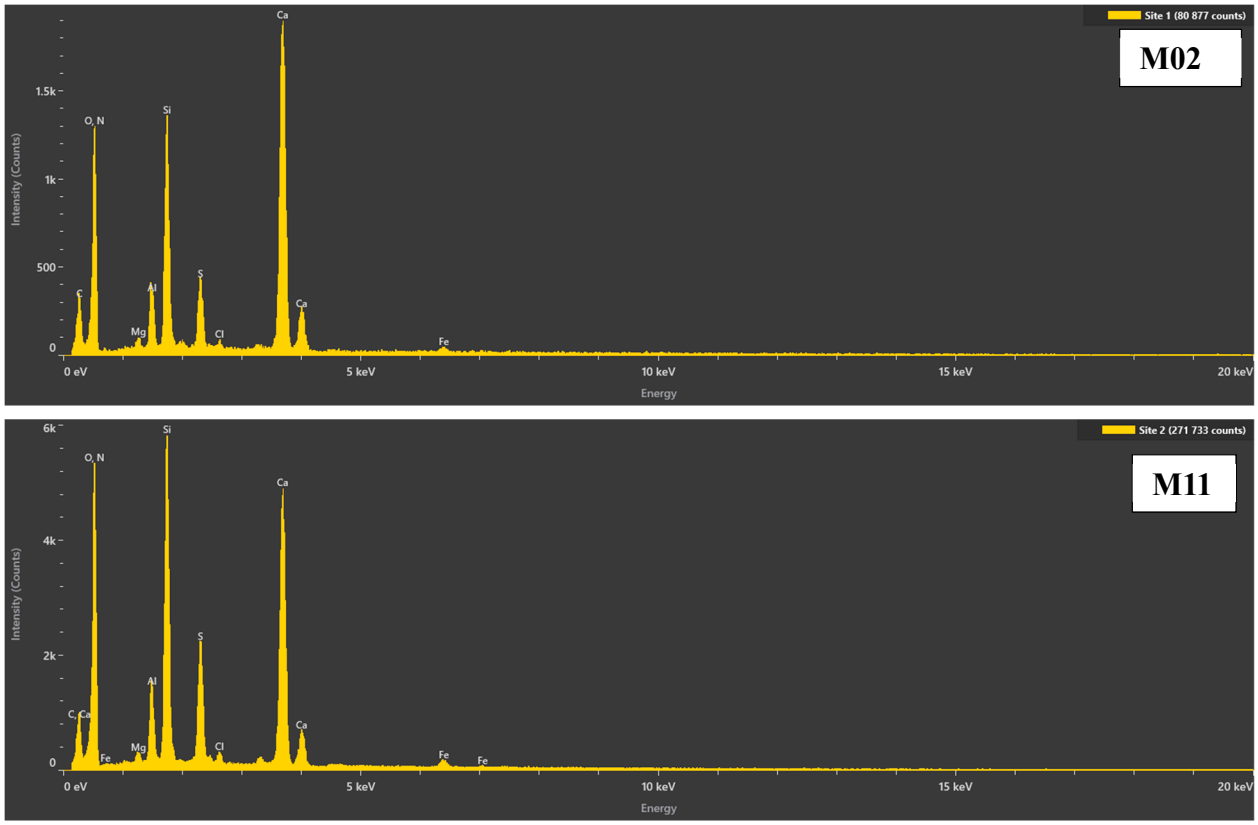

Figure 15. EDS test results for the M02 and M11 samples.

4. Conclusions

This study investigated the efficacy of a composite binder comprising cement bypass dust (CBD) and spent fluid catalytic cracking (FCC) catalyst for sustainable pavement base stabilization. The research yielded several significant findings:

1. The 50% FCC:50% CBD mixture demonstrated superior performance, achieving unconfined compressive strength (UCS) values of 15.6 MPa at 28 days with 10% binder content. This synergistic effect is attributed to the balanced pozzolanic and cementitious reactions.
2. UCS values exhibited consistent increases with higher binder content and longer curing periods. The 10% binder content samples showed the most significant strength gains, with UCS values ranging from 6.7 Mpa at 3 days to 15.6 MPa at 28 days.
3. Analysis of stress–strain curves revealed increasing E50 modulus values with higher binder content and curing time. For the optimal mix, E50 values ranged from 5025 MPa at 3 days to 13,922 MPa at 28 days for 10% binder content, indicating substantial improvement in material stiffness.
4. Higher binder contents (8–10%) demonstrated enhanced resistance to degradation during wetting–drying cycles, indicating improved long-term performance under variable environmental conditions.
5. SEM, XRD, and EDS analyses revealed a denser matrix with improved particle binding in samples with higher binder content, corroborating the enhanced mechanical properties.
6. The utilization of CBD and FCC, industrial by-products, in pavement construction contributes to waste reduction and resource conservation, aligning with circular economy principles.

The optimal mix design of 10% binder content with a 50% CBD:50% FCC ratio offers a viable, sustainable alternative to traditional stabilizers for pavement base construction. This approach not only enhances mechanical properties and durability but also promotes cleaner production practices in road infrastructure development.

Future research should focus on field applications, long-term performance monitoring, and potential leaching behavior to further validate the efficacy and environmental safety of this stabilization method. The findings provide a foundation for developing more sustainable and resilient road infrastructure, addressing both environmental concerns and the need for durable pavement systems.

Author Contributions: Conceptualization, S.E.R.; methodology, M.Y.F.; software, S.E.R.; validation, M.Y.F., W.H.H. and M.H.; formal analysis, S.E.R. and M.Y.F.; investigation, S.E.R. and M.Y.F.; resources, M.Y.F.; data curation, S.E.R.; writing—original draft preparation, S.E.R.; writing—review and editing, S.E.R. and M.Y.F.; visualization, S.E.R. and M.Y.F.; supervision, W.H.H. and M.Y.F.; project administration, W.H.H. and M.Y.F.; funding acquisition, S.E.R., M.Y.F., W.H.H. and M.H. All authors have read and agreed to the published version of the manuscript.

Funding: This research received no external funding.

Data Availability Statement: The datasets presented in this article are not readily available because the data are part of an ongoing PhD study. Requests to access the datasets should be directed to sajjad.e@uokerbala.edu.iq

Conflicts of Interest: The authors have no conflicts of interest.

Nomenclature

Symbol	Description
CBD	Cement Bypass Dust
FCC	Spent Fluid Catalytic Cracking Catalyst
UGB	Unbound Granular Base
XRF	X-Ray Fluorescence
XRD	X-Ray Diffraction
SEM	Scanning Electron Microscopy
OMC	Optimum Moisture Content
MDD	Maximum Dry Density
CBR	California Bearing Ratio
UCS	Unconfined Compressive Strength
SO_3	Sulfur Trioxide
TSS	Total Soluble Salts
L.A.	Los Angeles
CaO	Calcium Oxide
SiO_2	Silicon Dioxide
K_2O	Potassium Oxide
Fe_2O_3	Iron Oxide
Al_2O_3	Aluminum Oxide
TiO_2	Titanium Dioxide
La_2O_3	Lanthanum Oxide
Y	Zeolite Y
FWHM	Full-Width at Half-Maximum
EDS	Energy-Dispersive X-ray Spectroscopy

References

1. Mohammadinia, A.; Arulrajah, A.; D'Amico, A.; Horpibulsuk, S. Alkali-activation of fly ash and cement kiln dust mixtures for stabilization of demolition aggregates. *Constr. Build. Mater.* **2018**, *186*, 71–78. [CrossRef]
2. Gautam, P.K.; Kalla, P.; Jethoo, A.S.; Agrawal, R.; Singh, H. Sustainable use of waste in flexible pavement: A review. *Constr. Build. Mater.* **2018**, *180*, 239–253. [CrossRef]
3. Mohajerani, A.; Burnett, L.; Smith, J.V.; Markovski, S.; Rodwell, G.; Rahman, M.T.; Kurmus, H.; Mirzababaei, M.; Arulrajah, A.; Horpibulsuk, S.; et al. Recycling waste rubber tyres in construction materials and associated environmental considerations: A review. *Resour. Conserv. Recycl.* **2020**, *155*, 104679. [CrossRef]
4. Elliot, T.; Carter, A.; Ghattuwar, S.; Levasseur, A. Environmental impacts of road pavement rehabilitation. *Transp. Res. Part D Transp. Environ.* **2023**, *118*, 103720. [CrossRef]

5. Balaguera, A.; Carvajal, G.I.; Albertí, J.; Fullana-i-Palmer, P. Life cycle assessment of road construction alternative materials: A literature review. *Resour. Conserv. Recycl.* **2018**, *132*, 37–48. [CrossRef]
6. Arulrajah, A.; Disfani, M.M.; Horpibulsuk, S.; Suksiripattanapong, C.; Prongmanee, N. Physical properties and shear strength responses of recycled construction and demolition materials in unbound pavement base/subbase applications. *Constr. Build. Mater.* **2014**, *58*, 245–257. [CrossRef]
7. Chong, D.; Wang, Y. Impacts of flexible pavement design and management decisions on life cycle energy consumption and carbon footprint. *Int. J. Life Cycle Assess.* **2017**, *22*, 952–971. [CrossRef]
8. Hossain, M.U.; Poon, C.S.; Lo, I.M.C.; Cheng, J.C.P. Comparative environmental evaluation of aggregate production from recycled waste materials and virgin sources by LCA. *Resour. Conserv. Recycl.* **2016**, *109*, 67–77. [CrossRef]
9. Gulotta, T.M.; Mistretta, M.; Praticò, F.G. A life cycle scenario analysis of different pavement technologies for urban roads. *Sci. Total Environ.* **2019**, *673*, 585–593. [CrossRef]
10. Zhang, J.; Li, C.; Ding, L.; Li, J. Performance evaluation of cement stabilized recycled mixture with recycled concrete aggregate and crushed brick. *Constr. Build. Mater.* **2021**, *296*, 123596. [CrossRef]
11. Wang, T.; Xiao, F.; Zhu, X.; Huang, B.; Wang, J.; Amirkhanian, S. Energy consumption and environmental impact of rubberized asphalt pavement. *J. Clean. Prod.* **2018**, *180*, 139–158. [CrossRef]
12. Abd El-Aleem, S.; Abd-El-Aziz, M.A.; Heikal, M.; El Didamony, H. Effect of cement kiln dust substitution on chemical and physical properties and compressive strength of portland and slag cements. *Arab. J. Sci. Eng.* **2005**, *30*, 263–273.
13. Czapik, P.; Zapała-Sławeta, J.; Owsiak, Z.; Stępień, P. Hydration of cement by-pass dust. *Constr. Build. Mater.* **2020**, *231*, 117139. [CrossRef]
14. Adaska, W.S.; Taubert, D.H. Beneficial uses of cement kiln dust. *IEEE Cem. Ind. Tech. Conf.* **2008**, 210–228. [CrossRef]
15. Sreekrishnavilasam, R.A.; Santagata, M.C. *Development of Criteria for the Utilization of Cement Kiln Dust (CKD) in Highway Infrastructures*; Purdue University: West Lafayette, IN, USA, 2006.
16. Taha, R.; Al-Rawas, A.; Al-Harthy, A.; Al-Siyabi, H. Use of cement by-pass dust in soil stabilization. *Eng. J. Univ. Qatar* **2001**, *14*, 61–76.
17. Taha, R.; Al-Rawas, A.; Al-Harthy, A.; Qatan, A. Use of Cement Bypass Dust as Filler in Asphalt Concrete Mixtures. *J. Mater. Civ. Eng.* **2002**, *14*, 338–343. [CrossRef]
18. Owsiak, Z.; Czapik, P.; Zapała-Sławeta, J. Properties of a three-component mineral road binder for deep-cold recycling technology. *Materials* **2020**, *13*, 3585. [CrossRef]
19. Kalina, L.; Bílek, V.; Kiripolský, T.; Novotný, R.; Másilko, J. Cement kiln by-pass dust: An effective alkaline activator for pozzolanic materials. *Materials* **2018**, *11*, 1770. [CrossRef]
20. Hanein, T.; Hayashi, Y.; Utton, C.; Nyberg, M.; Martinez, J.C.; Quintero-Mora, N.I.; Kinoshita, H. Pyro processing cement kiln bypass dust: Enhancing clinker phase formation. *Constr. Build. Mater.* **2020**, *259*, 120420. [CrossRef]
21. Vojvodíková, B.; Procházka, L.; Bohácová, J. X-ray diffraction of alkali-activated materials with cement by-pass dust. *Crystals* **2021**, *11*, 782. [CrossRef]
22. Ferella, F.; Innocenzi, V.; Maggiore, F. Oil refining spent catalysts: A review of possible recycling technologies. *Resour. Conserv. Recycl.* **2016**, *108*, 10–20. [CrossRef]
23. Rodríguez, E.D.; Bernal, S.A.; Provis, J.L.; Gehman, J.D.; Monzó, J.M.; Payá, J.; Borrachero, M.V. Geopolymers based on spent catalyst residue from a fluid catalytic cracking (FCC) process. *Fuel* **2013**, *109*, 493–502. [CrossRef]
24. Marafi, M.; Stanislaus, A.; Furimsky, E. *Handbook of Spent Hydroprocessing Catalysts: Regeneration, Rejuvenation, Reclamation, Environment and Safety*; Elsevier: Amsterdam, The Netherlands, 2010; ISBN 9780444535566.
25. Payá, J.; Monzó, J.; Borrachero, M.V. Fluid catalytic cracking catalyst residue (FC3R): An excellent mineral by-product for improving early-strength development of cement mixtures. *Cem. Concr. Res.* **1999**, *29*, 1773–1779. [CrossRef]
26. Anh Le, T.; Hoang Le, S.; Ninh Nguyen, T.; Tan Nguyen, K. Assessment of the rheological and mechanical properties of geopolymer concrete comprising fly ash and fluid catalytic cracking residue as aluminosilicate precursor. *Appl. Sci.* **2021**, *11*, 3032. [CrossRef]
27. Dimulescu, C.; Burlacu, A. Industrial waste materials as alternative fillers in asphalt mixtures. *Sustainability* **2021**, *13*, 8068. [CrossRef]
28. Zhang, D.; Fang, S.; Zhang, H.; Liu, Z.; Zhang, Z.; Zhang, S. Utilization of Spent FCC Catalyst as Fine Aggregate in Non-sintered Brick: Alkali Activation and Environmental Risk Assessment. *Front. Chem.* **2021**, *9*, 674271. [CrossRef]
29. Xue, Y.; Wei, X.; Zhao, H.; Wang, T.; Xiao, Y. Interaction of spent FCC catalyst and asphalt binder: Rheological properties, emission of VOCs and immobilization of metals. *J. Clean. Prod.* **2020**, *259*, 120830. [CrossRef]
30. Kong, L.; Li, X.; He, S.; Wu, C.; Peng, Y.; Wang, H.; Shao, Q.; Zhang, A.A. Study on the influence of spent-catalysts microphysical properties on FCC/asphalt interface interaction. *Intell. Transp. Infrastruct.* **2023**, *2*, liad027. [CrossRef]
31. Li, J.; Shen, W.; Zhang, B.; Ji, X.; Chen, X.; Ma, W.; Hu, J.; Zhou, M.; Li, Y. Investigation on the preparation and performance of clinker-fly ash-gypsum road base course binder. *Constr. Build. Mater.* **2019**, *212*, 39–48. [CrossRef]
32. Limbachiya, V.; Ganjian, E.; Claisse, P. The impact of variation in chemical and physical properties of PFA and BPD semi-dry cement paste on strength properties. *Constr. Build. Mater.* **2015**, *96*, 248–255. [CrossRef]
33. Collins, R.J.; Emery, J. *Kiln Dust-Fly Ash Systems for Highway Bases and Subbases*; Federal Highway Administration: Washington, DC, USA, 1983.

34. Ministry of Housing and Construction. *Iraqi Standard Specifications for Roads and Bridges*; Ministry of Housing and Construction: Baghdad, Iraq, 2003.
35. *BS 1377-3:2018+A1:2021*; Methods of Test for Soils for Civil Engineering Purposes–Chemical and Electro-Chemical Testing. British Standards Institution: London, UK, 2021.
36. *ASTM D2974-20*; Standard Test Methods for Determining the Water (Moisture) Content, Ash Content, and Organic Material of Peat and Other Organic Soils. ASTM International: West Conshohocken, PA, USA, 2020.
37. *AASHTO T89-68*; Standard Method of Test for Determining the Liquid Limit of Soils. American Association of State Highway and Transportation Officials: Washington, DC, USA, 1968.
38. *AASHTO T90-70*; Standard Method of Test for Determining the Plastic Limit and Plasticity Index of Soils. American Association of State Highway and Transportation Officials: Washington, DC, USA, 1970.
39. *ASTM D1883-16*; Standard Test Method for California Bearing Ratio (CBR) of Laboratory-Compacted Soils. ASTM International: West Conshohocken, PA, USA, 2016.
40. *ASTM C131/C131M-20*; Standard Test Method for Resistance to Degradation of Small-Size Coarse Aggregate by Abrasion and Impact in the Los Angeles Machine. ASTM International: West Conshohocken, PA, USA, 2020.
41. *ASTM D1557-12(2021)*; Standard Test Methods for Laboratory Compaction Characteristics of Soil Using Modified Effort (56,000 ft-lbf/ft^3 (2,700 kN-m/m^3)). ASTM International: West Conshohocken, PA, USA, 2021.
42. *ASTM D1633M*; Standard Test Methods for Compressive Strength of Molded Soil-Cement Cylinders. ASTM International: West Conshohocken, PA, USA, 2017.
43. *ASTM D559/D559M-15*; Standard Test Methods for Wetting and Drying Compacted Soil-Cement Mixtures. ASTM International: West Conshohocken, PA, USA, 2015. [CrossRef]
44. Antiohos, S.K.; Papadakis, V.G.; Chaniotakis, E.; Tsimas, S. Improving the performance of ternary blended cements by mixing different types of fly ashes. *Cem. Concr. Res.* **2007**, *37*, 877–885. [CrossRef]
45. Pacewska, B.; Wilińska, I.; Bukowska, M. Hydration of cement slurry in the presence of spent cracking catalyst. *J. Therm. Anal. Calorim.* **2000**, *60*, 71–78. [CrossRef]
46. Garcés, P.; Pérez Carrión, M.; García-Alcocel, E.; Payá, J.; Monzó, J.; Borrachero, M.V. Mechanical and physical properties of cement blended with sewage sludge ash. *Waste Manag.* **2008**, *28*, 2495–2502. [CrossRef] [PubMed]
47. Sadique, M.; Al Nageim, H.; Atherton, W.; Seton, L.; Dempster, N. A new composite cementitious material for construction. *Constr. Build. Mater.* **2012**, *35*, 846–855. [CrossRef]
48. Chindaprasirt, P.; Jaturapitakkul, C.; Sinsiri, T. Effect of fly ash fineness on microstructure of blended cement paste. *Constr. Build. Mater.* **2007**, *21*, 1534–1541. [CrossRef]
49. Lim, S.; Zollinger, D.G. Estimation of the Compressive Strength and Modulus of Elasticity of Cement-Treated Aggregate Base Materials. *Transp. Res. Rec.* **2003**, *1837*, 30–38. [CrossRef]
50. Xiao, J.; Qiang, C.; Nanni, A.; Zhang, K. Use of sea-sand and seawater in concrete construction: Current status and future opportunities. *Constr. Build. Mater.* **2017**, *155*, 1101–1111. [CrossRef]
51. Ghanizadeh, A.R.; Rahrovan, M.; Bafghi, K.B. The effect of cement and reclaimed asphalt pavement on the mechanical properties of stabilized base via full-depth reclamation. *Constr. Build. Mater.* **2018**, *161*, 165–174. [CrossRef]
52. Al-Dossary, A.A.S.; Awed, A.M.; Gabr, A.R.; Fattah, M.Y.; El-Badawy, S.M. Performance enhancement of road base material using calcium carbide residue and sulfonic acid dilution as a geopolymer stabilizer. *Constr. Build. Mater.* **2023**, *364*, 129959. [CrossRef]
53. Horpibulsuk, S.; Rachan, R.; Chinkulkijniwat, A.; Raksachon, Y.; Suddeepong, A. Analysis of strength development in cement-stabilized silty clay from microstructural considerations. *Constr. Build. Mater.* **2010**, *24*, 2011–2021. [CrossRef]
54. Puppala, A.J.; Hoyos, L.R.; Potturi, A.K. Resilient Moduli Response of Moderately Cement-Treated Reclaimed Asphalt Pavement Aggregates. *J. Mater. Civ. Eng.* **2011**, *23*, 990–998. [CrossRef]
55. Arifin, Y.F.; Agustina, E.; Andhi, F.; Agus, S.S. The role of additives in soil-cement subjected to wetting-drying cycles. *Infrastructures* **2021**, *6*, 48. [CrossRef]
56. Zhang, H.; Cheng, Y.; Yang, L.; Song, W. Modification of lime-fly ash-crushed stone with phosphogypsum for road base. *Adv. Civ. Eng.* **2020**, *2020*, 8820522. [CrossRef]
57. Rasul, J.M.; Ghataora, G.S.; Burrow, M.P.N. The effect of wetting and drying on the performance of stabilized subgrade soils. *Transp. Geotech.* **2018**, *14*, 1–7. [CrossRef]
58. Avirneni, D.; Peddinti, P.R.T.; Saride, S. Durability and long term performance of geopolymer stabilized reclaimed asphalt pavement base courses. *Constr. Build. Mater.* **2016**, *121*, 198–209. [CrossRef]
59. Chen, J.J.; Thomas, J.J.; Taylor, H.F.W.; Jennings, H.M. Solubility and structure of calcium silicate hydrate. *Cem. Concr. Res.* **2004**, *34*, 1499–1519. [CrossRef]
60. Wolter, J.M.; Schmeide, K.; Huittinen, N.; Stumpf, T. Cm(III) retention by calcium silicate hydrate (C-S-H) gel and secondary alteration phases in carbonate solutions with high ionic strength: A site-selective TRLFS study. *Sci. Rep.* **2019**, *9*, 14255. [CrossRef]
61. Dhanasekaran, V.; Mahalingam, T.; Chandramohan, R. Post Heat Treatment Effect on Electrochemically Synthesized CuO Thin Films. *ECS Trans.* **2013**, *45*, 73–78. [CrossRef]

62. Madadi, A.; Wei, J. Characterization of Calcium Silicate Hydrate Gels with Different Calcium to Silica Ratios and Polymer Modifications. *Gels* **2022**, *8*, 75. [CrossRef]
63. Fan, M.X.; Chen, F.X.; Zhang, X.Y.; Wang, R.K.; Yu, R. Effect of Ca/Si ratio on the characteristics of alkali-activated ultra-high performance concrete (A-UHPC): From hydration kinetics to microscopic structure development. *Constr. Build. Mater.* **2023**, *394*, 132158. [CrossRef]